small NANO MICRO

Gold nanoparticles

Preparation of Stable Maleimide-Functionalized Au Nanoparticles and Their Use in Counting Surface Ligands**

*E. Oh, K. Susumu, J. B. Blanco-Canosa, I. L. Medintz, P. E. Dawson, and H. Mattoussi**

It has long been known that maleimide reaction with sulfhydryl groups is highly efficient and provides a stable linkage.[1,2] Maleimide coupling to cysteine thiols is one of the most common bioconjugation techniques for labeling DNA, proteins, and peptides with organic fluorophores, due to the efficiency of the chemical reaction and its site specificity.[2,3] In addition, this coupling reaction has little or no effect on the biological activity of the target biomolecule.[2] This coupling strategy has also been applied to conjugate thiol-reactive polymers with peptides and proteins,[4,5] and was used to attach peptides and carbohydrates onto gold surface self-assembled monolayers;[6] in the latter example, the monolayers were used as biochips to probe enzymatic phosphorylation and to pattern mammalian cells. These key advantages have motivated the expansion of this coupling strategy to inorganic nanocrystals and polymeric nanoparticles, as it allows site-specific attachment of nanoprobes to target proteins and peptides.[7,8] For example, maleimide-functionalized 1.4-nm-size gold nanoparticles (AuNPs) are commercially available (Nanoprobes, Inc.) and have been used in several studies.[9–12]

Use of colloidal inorganic nanocrystals has gained tremendous interest in the past decade, driven by the ever increasing range of potential applications in and outside biology.[9,13–18] These NPs are often functionalized with surface ligands to promote their dispersion in aqueous solution.[13,14,18] Attaching end reactive groups onto the ligands allows coupling of these nanoprobes to target biomolecules. Moreover, quantitative control of the surface functionalities would further expand the use of these materials and enhance their utility in biology. For NPs (metallic, semiconducting, and magnetic) made dispersible via organic capping ligands, the number or density of ligands on the NP surfaces is crucial to controlling their functionality. Such information could allow better understanding of the ligand contribution to crucial properties such as colloidal stability, passivation of the surface electronic states (e.g., luminescent quantum dots) and reactivity of the NPs. There have been several studies aimed at determining the number of ligands capping the surface of inorganic nanocrystals, including those made of metallic, semiconducting, and magnetic materials.[19–22] Often the reported analytical approaches are faced with experimental constraints such as affinity of the ligands to the inorganic surface of the NPs, difficulty to avoid/reduce non-specific interactions, and the uncertainties associated with the reporting signals such as absorption, fluorescence, NMR, or electron paramagnetic resonance (EPR) measurements. This makes it highly desirable to implement counting strategies using new ligands that exhibit high affinity to the NP surfaces and that are compatible with strong coupling strategies. This can also improve the available ligand-counting methods and complement the results already reported in the literature.

Here we describe the design and synthesis of a modular ligand made of a thioctic acid (TA)-appended poly(ethylene glycol) (PEG) end-functionalized with a maleimide group (TA-PEG-Mal), and its use to prepare maleimide-functionalized AuNPs (see schematics in Figure 1). We show that control over the fraction of TA-PEG-Mal ligands on the NPs allows us to estimate the number of surface ligands on AuNPs. For this, AuNPs of different sizes (10-nm and 15-nm nominal diameters from Ted Pella) were cap-exchanged with varying fractions of TA-PEG-Mal mixed with an inert ligand made of methoxy-terminated TA-PEG (TA-PEG-OCH_3).[23] The AuNPs functionalized with TA-PEG-Mal, hereafter referred to as Mal-AuNPs, were reacted with the terminal cysteine on a peptide sequence, then to Cy5 dye, creating AuNP-Mal-Pep-Cy5 assemblies. Using different TA-PEG-Mal fractions allowed

[*] Prof. H. Mattoussi
Florida State University
Department of Chemistry and Biochemistry
Tallahassee, FL 32306 (USA)
E-mail: mattoussi@chem.fsu.edu
Dr. E. Oh, Dr. K. Susumu, Dr. I. L. Medintz, Prof. H. Mattoussi
US Naval Research Laboratory
Division of Optical Sciences
Washington, DC 20375 (USA)
Dr. J. B. Blanco-Canosa, Prof. P. E. Dawson
Departments of Cell Biology & Chemistry
The Scripps Research Institute
La Jolla, CA 92037 (USA)

[**] The authors acknowledge NRL, ONR, and DTRA and NIH for financial support. E.O. was supported by a fellowship from the Korea Research Foundation (D00089). J.B.B.-C. acknowledges the Marie Curie Program for a postdoctoral fellowship.

Supporting Information is available on the WWW under http://www.small-journal.com or from the authors

DOI: 10.1002/smll.201000279

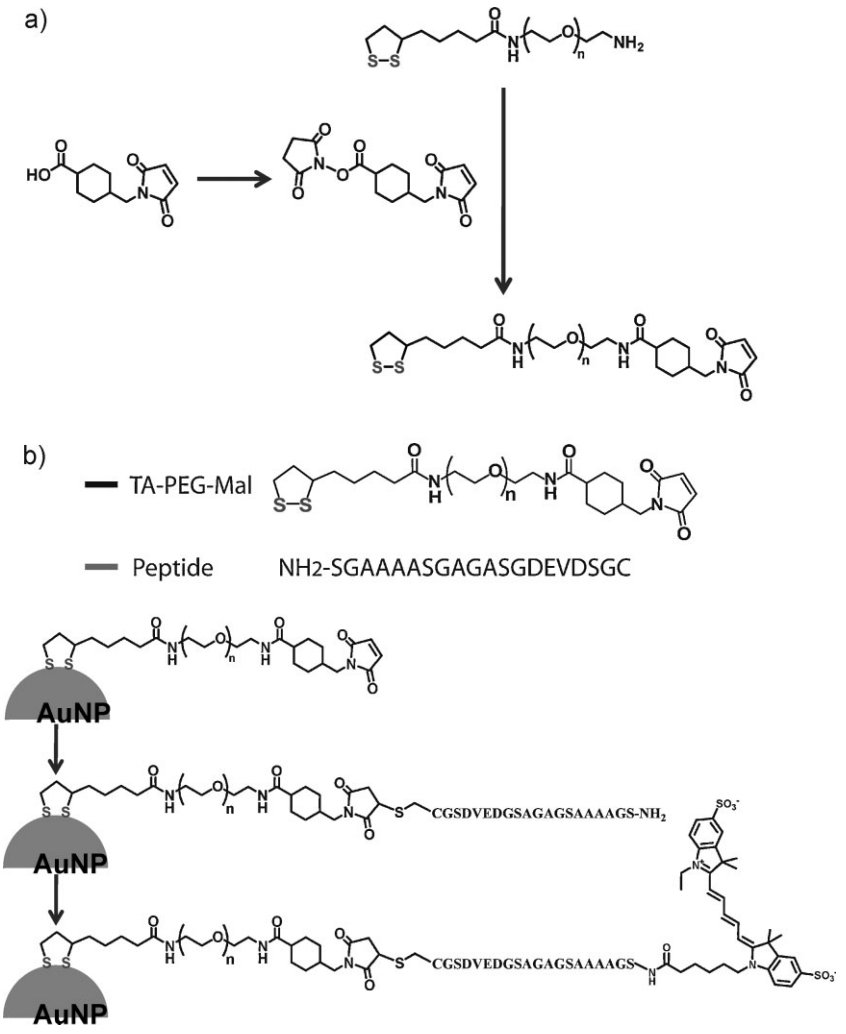

Figure 1. a) Scheme for preparing TA-PEG-Mal ligand. b) Schematic representation of TA-PEG-Mal-capped AuNPs and the ensuing coupling reactions to attach peptide then Cy5 dye to the NPs. Further details on the synthesis and purification of TA-PEG-Mal are provided in the Experimental Section.

coupling of varying numbers of peptide-Cy5 on each AuNP. Cy5 was chosen because its absorption peak was optically distinguishable from the surface plasmon resonance band (SPB) of the AuNPs. Changes in the Cy5 absorbance were then used to extract the number of peptide-dye per AuNP for each TA-PEG-Mal fraction. Tracking the dependence of the number of peptide-Cy5 per AuNP on TA-PEG-Mal fraction provided the total number (and the density) of TA-PEG ligands on the NPs.

We further examined the long-term stability of our Mal-AuNPs and AuNP-Mal-Pep conjugates in the presence of excess electrolyte and dithiothreitol (DTT). In particular, we compared the colloidal stability of our maleimide-functionalized AuNPs to commercially available 1.4-nm monomaleimide AuNPs (Nanoprobes, Inc.) as well as our AuNP-peptide conjugates to AuNP-Cys-Pep assemblies prepared via direct adsorption of thiol-terminated peptides onto the NPs; this method has been traditionally employed for assembling AuNP-peptide and AuNP-oligonucleotide conjugates.[20,24,25]

AuNPs with different TA-PEG-Mal fractions (0, 5, 10, 20, and 30%) were prepared via surface-ligand exchange of citrate-stabilized AuNPs (TedPella, Inc.) using mixtures of TA-PEG-Mal and inert TA-PEG-OCH_3.[23] Because the two sets of ligands have identical anchoring groups (TA) and PEG segments with similar lengths, the fraction of maleimide groups on the final AuNPs is expected to be the same as that used in the cap-exchange mixture.[23] The nanoparticles were then reacted with the terminal cysteine on a peptide retaining an unblocked primary amine at its other terminus (NH_2-SGA-AAASGAGASGDEVDSGC), using a peptide-to-Au surface atom ratio of 2 (large excess of peptide). Following purification from excess free peptide using PD-10 desalting column (GE Healthcare Life Sciences), the AuNP-Mal-Pep conjugates were further reacted with excess NHS-functionalized Cy5; the NHS-dye directly coupled to the available terminal amine.[2] For this coupling step we used a nanoparticle concentration of ≈2–20 nM and a large molar excess of NHS-Cy5 (dye-to-Au surface ratio ≈20).

We then characterized the optical properties of these AuNP-Mal-Pep-Cy5 dispersions after purification using a PD-10 column and determined the number of TA-PEG-Mal groups on the AuNP surfaces. The absorption spectra collected from dispersions of Mal-AuNPs coupled to peptide-Cy5 show a contribution characteristic of the Cy5 dye (absorption bands at ≈600 and ≈650 nm) that increases with increasing Mal fractions on the NP (Figure 2A). The net contribution of the Cy5 conjugated to AuNPs was obtained by subtracting the absorbance of the original Mal-AuNPs from those of the AuNP-Mal-Pep-Cy5 dispersions (Figure 2A, inset). Using the dye extinction coefficient ($2.5 \times 10^5\ M^{-1}\ cm^{-1}$ at 649 nm, provided by the manufacturer) we estimated the molar concentration of Cy5 coupled to AuNPs in the sample. The number of peptide-dye per AuNP was then calculated by normalizing the Cy5 concentration to that of the AuNPs; the latter was extracted from the absorption spectra of the AuNP dispersions using the extinction coefficient at 520 nm for each NP size (provided by the manufacturer): $9.6 \times 10^7\ M^{-1}\ cm^{-1}$ for 10-nm AuNPs and $36 \times 10^7\ M^{-1}\ cm^{-1}$ for 15-nm AuNPs, respectively. Figure 2B shows a plot of the number of peptide-dye versus fraction of Mal groups per AuNP for the two sets of NPs used. Data show that there is a linear increase in the number of peptide-Cy5 with Mal fraction. This indicates that the cap exchange with different fractions of mixed ligands can allow control over the number of end-functionalized ligands per AuNP. Nonetheless, data also show that there is a finite number of peptide-dye attached to the AuNPs without TA-PEG-Mal (0% Mal). This can be attributed to two factors: i) direct binding of the terminal cysteine of the peptide onto the

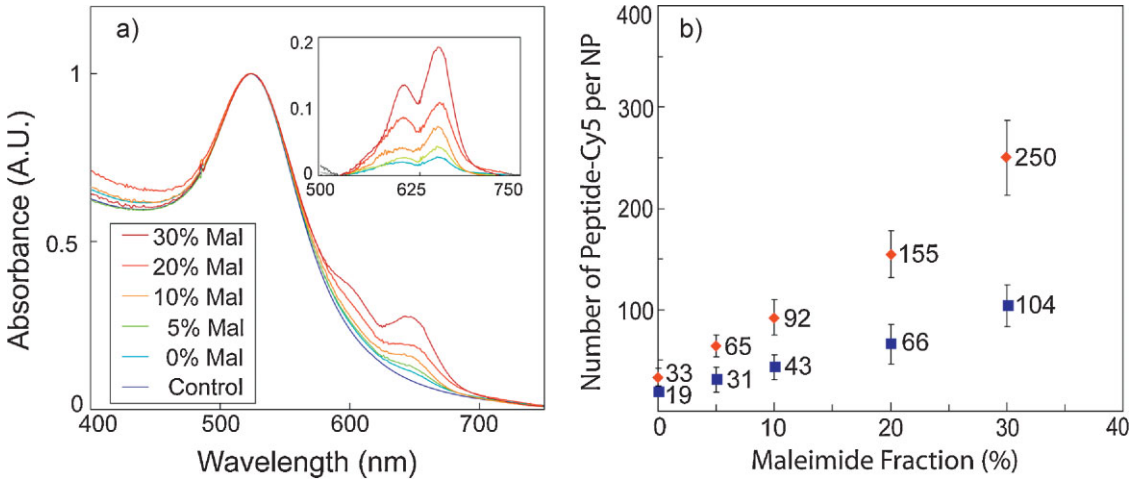

Figure 2. a) UV/vis absorption spectra of 15-nm Mal-AuNPs (control) and AuNP-Mal-Pep-Cy5 for different fractions of TA-PEG-Mal on a NP. Inset shows the net spectra of Cy5 extracted from the raw data. b) Number of peptide-Cy5 per AuNP for each Mal fraction for 10-nm (blue square) and 15-nm AuNPs (red diamond).

Au surface and/or ii) non-specific adsorption of Cy5 on the NP surface. Subtracting the value at 0% Mal provided a measure for the net number of peptide-dye at each maleimide fraction (see Table 1). In Table 1, we also report the total number of surface ligands for complete coverage (extracted from extrapolation at 100% Mal ligands) for both sets of NPs. In this analysis, we assumed 1) the AuNPs are spherical in shape; 2) homogeneous distribution of ligands on the NP surface; 3) the two successive coupling reactions (Mal-to-cysteine and amine to NHS-dye) are 100% efficient and produce Cy5 labeling of all maleimide groups on the nanoparticles. However, these reactions obey binary molecular interactions and their efficiency depends on the substrate concentration (here the AuNP-Mal) and the molar ratios between Mal and peptide and between Mal-peptide and Cy5; large ratios (excess peptide and dye) were used in both reactions to maximize the labeling efficiency. Nonetheless, given the fact that we have performed Cy5 coupling to the nanoparticles in two steps (peptide to maleimide on the AuNP followed by dye conjugation to the peptide), our labeling strategy may imply that the final number of Cy5 groups per NP extracted is always underestimated. An alternative option could use a pre-labeled peptide, which could then be coupled to the maleimide on the NP.[22]

The apparent footprint area (FPA) per ligand, defined as the average area occupied by a ligand on the NP surface, is 1.20 ± 0.08 and $1.27 \pm 0.10\,nm^2$ for 10-nm and 15-nm AuNPs, respectively (see Table 1). The consistent FPA values extracted for both NP sizes indicate that the distribution of ligands on the NP surface is indeed homogeneous. These FPA values are larger than those previously reported for 2.8-nm AuNPs capped with monothiol-PEG ligands using thermal gravimetric analysis ($FPA \approx 0.35\,nm^2$).[19] Alternatively, one could use the density of ligand coverage, also reported as percentage of surface Au atoms on the NP surface occupied by ligands (Table 1). These experiments indicate that a larger FPA, or lower density of ligand coverage, is measured for our bidentate TA-PEG ligands, with about a factor of 2.5 difference. The larger footprint area (or smaller coverage) can be primarily attributed to the larger size of TA anchoring group. Additional effects of PEG crowding for larger-sized NPs (smaller

Table 1. Values for net number of peptide-dye per AuNP along with the corresponding FPA extracted using the present strategy.

Size [nm]	% Maleimide	# of peptide	Net # of peptide[a]	# of ligand[b]	FPA [nm^2][c]	Thiol cov. [%][d]
10	0%	19 ± 4	–	–	–	–
	5%	31 ± 13	12	245	1.23	12
	10%	43 ± 12	24	245	1.23	12
	20%	66 ± 20	47	235	1.28	12
	30%	104 ± 21	85	284	1.06	14
15	0%	33 ± 9	–	–	–	–
	5%	65 ± 11	31	625	1.29	11
	10%	92 ± 17	59	589	1.36	11
	20%	155 ± 23	122	606	1.33	11
	30%	250 ± 37	216	722	1.11	13
2.8	–	–	–	–	0.35[e]	28[e]

[a] Net number of peptide-Cy5 = total number–the value at 0% maleimide. [b] Number of ligands = net number of peptide-Cy5/maleimide percentage. [c] FPA = surface area of AuNPs/total number of ligands. [d] Thiol coverage = (number of thiol groups)/(number of surface Au atoms). [e] Extracted from Reference [19] using thermogravimetric analysis.

curvature) and residual sodium citrate may also reduce ligand density.

We would like to distinguish our ligand-counting strategy from some of those reported in previous studies, which are often based on adsorbing thiol-terminated oligonucleotides or peptides onto citrate-stabilized AuNPs. Indeed, the net number of conjugated Cy5 dyes per AuNP we extracted at 30% Mal (e.g., ≈85 for 10 nm and ≈216 for 15 nm) is much larger than that reported for direct binding of thiol-modified 25-mer oligonucleotides onto citrate-stabilized AuNPs (≈68 for 10 nm and ≈110 for 15 nm, full surface coverage).[20] Another more direct comparison can be made with the number of peptide-dye extracted using an experimental design similar to ours described in Reference [22]. The authors used 32-nm AuNPs cap-exchanged with monothiol-PEG ligands, 14% of which were end-appended with amine groups. These amines were modified using a bifunctional maleimide-NHS linker, then dye-labeled cysteine-peptides were coupled to the maleimide groups. A value of 53 ligands was extracted for the amine-PEG ligands on the AuNPs from the dye optical characteristics following ligand removal from the NP surfaces. The net number of ligands extracted at 10% maleimide ≈60 (Table 1) is comparable to what was reported for 32-nm NP with 14% amine terminal groups (Reference [22]). However, normalizing the differences in NP surface area (32 nm NPs have ≈4 times larger surface area than their 15-nm counterparts) also indicates that a higher density of ligand coverage is measured for our samples. This difference may be the result of stronger affinity of the TA-PEG-maleimide ligand compared to monothiol modified ligands.

It is important to note that our ligand design offers another unique advantage, as it allows modification of the terminal amine of TA-PEG-NH_2 with maleimide prior to cap exchange on the AuNP. If maleimide transformation were applied to mono-thiol terminated ligands, chain reaction of maleimide with thiol groups would take place (head-to-tail) with free ligands, making it ineffective for capping AuNPs and coupling to target molecules. To circumvent this problem, monothiol-terminated ligands are first immobilized on the NP then coupled to a maleimide (e.g., via NHS bifunctional linkers), which adds another modification step to append the maleimides on the NPs.[7,22]

One of the key necessities for developing effective use of nanoprobes in biology is long-term stability under biological conditions. We tested the stability of our Mal-AuNPs and AuNP-Mal-Pep in the presence of 2 M NaCl and 0.5–1 M DTT. This concentration is much higher than those measured for thiol-containing molecules in biological environments; for example, intracellular glutathione concentration is only ≈10 mM.[26] DTT is known to have high affinity to Au surfaces due to its dithiol group. It is also one of the most common reagents used for reducing the disulfide bonds of biomolecules such as proteins, antibodies, or thiol-modified DNA.[2,27–29] At high concentration, DTT can effectively compete to bind to the AuNP surface, displacing the original ligands away from the NP and initiating aggregation.[30–33] We carried out stability tests of Mal-AuNPs side by side with 1.4-nm mono-maleimide nanogold surface-stabilized with tris(aryl)phosphine ligand (Nanoprobes, Inc.). We found that our Mal-AuNPs stayed stable and aggregate-free for at least 10 days in the presence of 2 M NaCl, while 1.4-nm commercial mono-maleimide AuNPs showed rapid precipitation (Figure 3). Similarly, adding 0.5 M DTT at pH 8 resulted in aggregate build-up and precipitation of commercial AuNPs within 10 minutes, while our Mal-AuNPs showed no signs of precipitation for extended periods of time (images of NP dispersions after 10 days of storage are shown in Figure 3). We also tested the stability of AuNP-peptide conjugates prepared via either maleimide-thiol coupling or direct adsorption of cysteine-peptide onto citrate-stabilized AuNPs (AuNP-Cys-Pep). A substantial difference between the

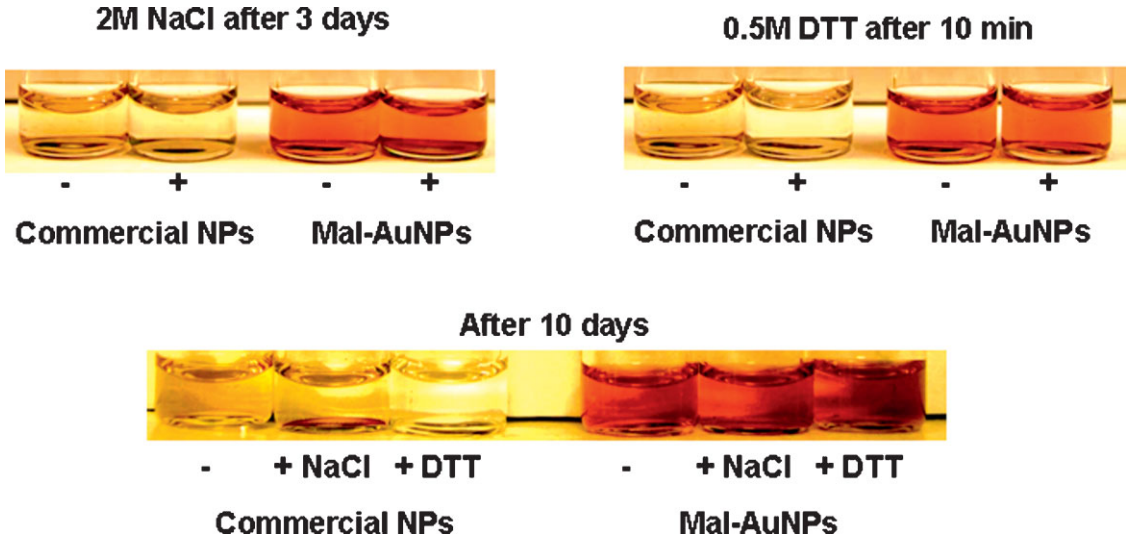

Figure 3. Side-by-side comparison of the dispersion stability for TA-PEG-Mal-capped 15-nm AuNPs and 1.4-nm commercial mono-maleimide-AuNPs. Top left) Dispersions without (–) and with (+) 2 M NaCl after 3 days of storage at room temperature. Top right) Dispersions without (–) and with (+) 0.5 M DTT at pH 8 after 10 min of storage at room temperature. Bottom) Dispersions without (–), with (+) 2 M NaCl, and with (+) 0.5 M DTT at pH 8 after 10 days of storage at room temperature. The rather weak SPB for 1.4-nm AuNPs produces weaker contrast, making rendition of the aggregate formation in the image rather poor.

two sets of NP dispersions was also observed. At pH 8, dispersions of AuNP-Cys-Pep completely precipitated within 5 min at room temperature in the presence of 0.8 M DTT and 0.8 M NaCl (Figure 4). In comparison, our AuNP-Mal-Pep were unaffected by added DTT, NaCl, and NaOH (Figure 4). These tests indicate that using TA-appended PEG ligands that present terminal maleimides for bioconjugation provides clear benefits, as the AuNPs and their conjugates exhibit enhanced stability to excess ions and to competition from DTT. The strong resistance to DTT competition is particularly promising for using the AuNPs to develop biological assays, which are often carried out in media containing thiol molecules such as cysteine, glutathione, mercaptoethanol, and DTT. The above DTT stability tests are more stringent than those carried out in biological media where the concentration of thiol-containing molecules is at least one to two orders of magnitude lower.

In summary, we designed and synthesized a set of PEG-based modular ligands presenting a disulfide anchoring group and a terminal maleimide function, and used them for the specific conjugation of AuNPs to peptides via maleimide-thiol coupling. By tuning the fraction of maleimide groups per NP we applied this system to estimate the number of surface ligands on each AuNP. Our approach demonstrated efficient conjugation of cysteine thiol on biomolecules to maleimide-functionalized AuNPs and the prepared AuNPs were stable for long periods of time even under ion- and thiol-rich conditions. These maleimide-functionalized AuNPs could find great utility in biology for designing plasmonic assays, intracellular delivery and tracking. We have, for example, coupled the present AuNP-Mal to thiol-functionalized biotin to prepare AuNP-biotin conjugates, and used them in a few preliminary colorimetric assays. Further details on these assays along with gel electrophoresis characterization of the AuNP-Mal-peptide conjugates are provided in the Supporting Information.

Experimental Section

Synthesis of TA-PEG600-maleimide: 4-(*N*-maleimidomethyl)cyclohexane-1-carboxylic acid (0.350 g, 1.48×10^{-3} mol), *N,N′*-dicyclohexylcarbodiimide (0.310 g, 1.50×10^{-3} mol), *N*-hydroxysuccinimide (0.200 g, 1.74×10^{-3} mol), triethylamine (0.20 ml, 1.4×10^{-3} mol), and CH_2Cl_2 (30 ml) were added to a 100-mL round-bottom flask, and the mixture was stirred for 1 h at room temperature under N_2. TA-PEG600-NH_2[34] (0.948 g, $\approx 1.22 \times 10^{-3}$ mol) in 10 mL of CH_2Cl_2 was added dropwise, and the reaction mixture was further stirred for 4 h. The reaction mixture was then filtered through celite, and the filtrate evaporated. The residue was chromatographed on silica gel initially with $CHCl_3$:MeOH (20:1) and then with $CHCl_3$:MeOH (10:1). Yield 0.238 g (≈20%). ^{1}H NMR (400 MHz, $CDCl_3$): δ (ppm) 6.71 (s, 2H, maleimide-H), 6.33 (br s, 1H, −CO−N*H*−), 6.19 (br s, 1H, −CO−N*H*−), 3.6–3.7 (m), 3.51–3.58 (m, 4H), 3.40–3.49 (m, 4H), 3.37 (d, 2H, $J = 6.8$ Hz), 3.08–3.22 (m, 2H), 2.42–2.52 (m, 1H), 2.20 (t, 2H, $J = 7.4$ Hz), 1.97–2.08 (m, 1H), 1.84–1.96 (m, 3H), 1.6–1.8 (m, 7H), 1.36–1.55 (m, 4H), 0.93–1.06 (m, 2H). Additional details on the NMR characterization of other TA-PEG-based ligands are provided in Reference [34].

Preparation of Mal-AuNPs: A mixture of TA-PEG-Mal and TA-PEG-OCH_3 at the desired Mal fraction was added to a citrate-stabilized AuNP dispersion (Ted Pella, Inc.) in de-ionized water at pH 7–7.5 and stirred for ≈8 h. The total ratio of ligand-to-Au surface atom used during the cap-exchange reaction was ≈200. The dispersion was then purified of free ligands by applying three cycles of concentration/dilution using a membrane filtration device (Millipore). The AuNPs were then stored at 4 °C until use.

Peptide conjugation to Mal-AuNPs: The peptides were first reduced by adding 10 mM of TCEP (tris(2-carboxyethyl)phosphine hydrochloride) with stirring for 1 h at room temperature. They were then reacted with Mal-AuNPs for 1 h at room temperature. The ratio of peptide to Au surface atom number used during the coupling reaction was ≈2. The dispersion was then purified from TCEP and the unreacted peptide using a PD-10 column with PBS as the eluting buffer. Characterization of the AuNP-peptide conjugates using gel electrophoresis is provided in the Supporting Information (Figure S1). The AuNP-Mal-Peptide assemblies were stored at 4 °C until use.

Cy5 labeling to AuNP-Mal-Pep: Cy5-NHS ester (GE healthcare life sciences) was dissolved in PBS buffer with 10% of 0.1 M

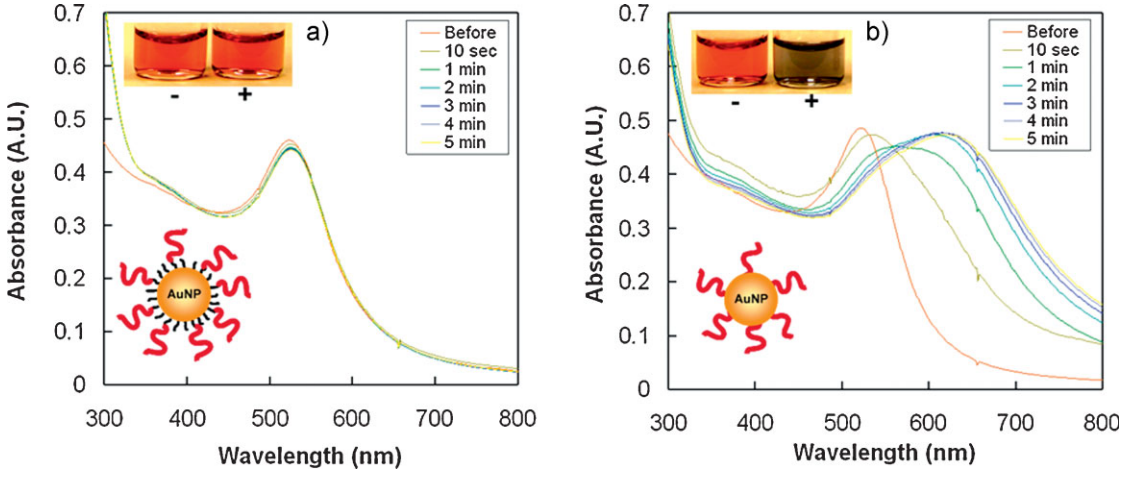

Figure 4. Time trace of the UV/vis absorption spectra of AuNP dispersions at pH 8 with 0.8 M DTT and 0.8 M NaCl: a) 10-nm AuNP-Mal-Pep and b) 10-nm AuNP-Cys-Pep. Insets show the images of AuNP dispersions without (–) and with (+) added DTT.

sodium borate, pH 7.5, added to AuNP-Mal-Pep dispersion and let react while stirring for 1 h. The ratio of Cy5 to Au surface atoms used was ≈20. The dispersion was then purified from free Cy5 on a PD-10 column using PBS as the eluting buffer. The absorption spectra were collected from these dispersions and used for further analysis.

Preparation of AuNP-Cys-Peptide conjugates (control): Commercial sodium citrate (SC) stabilized AuNPs (10 nm) were mixed with Cys-labeled peptide and stirred for 8 h. The molar ratio of peptide-to-Au surface atoms used during the coupling reaction was ≈2 (the same as used for preparing the AuNPs-Mal-Peptide above). The dispersions were then purified from free biomolecules using PD-10 column as described above and stored at 4 °C for further use.

Keywords:
gold nanoparticles · maleimide · peptides · sulfhydryl · surface ligands

[1] J. D. Gregory, *J. Am. Chem. Soc.* **1955**, *77*, 3922–3923.
[2] G. T. Hermanson, *Bioconjugate Techniques*, Academic Press, San Diego 2nd ed. **2008**.
[3] Y. Kim, S. O. Ho, N. R. Gassman, Y. Korlann, E. V. Landorf, F. R. Collart, S. Weiss, *Bioconjugate Chem.* **2008**, *19*, 786–791.
[4] G. Mantovani, F. Lecolley, L. Tao, D. M. Haddleton, J. Clerx, J. Cornelissen, K. Velonia, *J. Am. Chem. Soc.* **2005**, *127*, 2966–2973.
[5] Z. P. Tolstyka, J. T. Kopping, H. A. Maynard, *Macromolecules* **2008**, *41*, 599–606.
[6] B. T. Houseman, E. S. Gawalt, M. Mrksich, *Langmuir* **2003**, *19*, 1522–1531.
[7] S. J. Kuhn, S. K. Finch, D. E. Hallahan, T. D. Giorgio, *Nano Lett.* **2006**, *6*, 306–312.
[8] M. E. Gindy, S. X. Ji, T. R. Hoye, A. Z. Panagiotopoulos, R. K. Prud'homme, *Biomacromolecules* **2008**, *9*, 2705–2711.
[9] a) E. Katz, I. Willner, *Angew. Chem. Int. Ed.* **2004**, *43*, 6042 -L 6108; b) J. F. Hainfeld, F. R. Furuya, *J. Histochem. Cytochem.* **1992**, *40*, 177–184.
[10] R. A. McMillan, C. D. Paavola, J. Howard, l. S. Chan, N. J. Zaluzec, J. D. Trent, *Nat. Mater.* **2002**, *1*, 247–252.
[11] E. Chang, J. S. Miller, J. T. Sun, W. W. Yu, V. L. Colvin, R. Drezek, J. L. West, *Biochem. Biophys. Res. Commun.* **2005**, *334*, 1317–1321.
[12] T. Pons, I. L. Medintz, K. E. Sapsford, S. Higashiya, A. F. Grimes, D. S. English, H. Mattoussi, *Nano Lett.* **2007**, *7*, 3157–3164.
[13] M. C. Daniel, D. Astruc, *Chem. Rev.* **2004**, *104*, 293–346.
[14] P. K. Jain, X. Huang, I. H. El-Sayed, M. A. El-Sayed, *Acc. Chem. Res.* **2008**, *41*, 1578–1586.
[15] A. P. Alivisatos, *Nat. Biotechnol.* **2004**, *22*, 47–52.
[16] I. L. Medintz, H. T. Uyeda, E. R. Goldman, H. Mattoussi, *Nat. Mater.* **2005**, *4*, 435–446.
[17] *Nanobiotechnology II: More Concepts and Applications* (Eds.: C. A. Mirkin, C. M. Niemeyer) Wiley, Darmstadt, Germany **2007**.
[18] *Inorganic Nanoprobes for Biological Sensing and Imaging* (Eds.: H. Mattoussi, J. Cheon) Artech House, Norwood, MA **2009**.
[19] W. P. Wuelfing, S. M. Gross, D. T. Miles, R. W. Murray, *J. Am. Chem. Soc.* **1998**, *120*, 12696.
[20] H. D. Hill, J. E. Millstone, M. J. Banholzer, C. A. Mirkin, *ACS Nano* **2009**, *3*, 418–424.
[21] W. Liu, M. Howarth, A. B. Greytak, Y. Zheng, D. G. Nocera, A. Y. Ting, M. G. Bawendi, *J. Am. Chem. Soc.* **2008**, *130*, 1274–1284.
[22] L. Maus, J. P. Spatz, R. Fiammengo, *Langmuir* **2009**, *25*, 7910–7917.
[23] B. C. Mei, K. Susumu, I. L. Medintz, J. B. Delehanty, T. J. Mountziaris, H. Mattoussi, *J. Mater. Chem.* **2008**, *18*, 4949–4958.
[24] D. Zanchet, C. M. Micheel, W. J. Parak, D. Gerion, A. P. Alivisatos, *Nano Lett.* **2001**, *1*, 32–35.
[25] P. C. Patel, D. A. Giljohann, D. S. Seferos, C. A. Mirkin, *Proc. Natl. Ac. Sci. USA* **2008**, *105*, 17222–17226.
[26] Z. Z. Shi, J. Osei-Frimpong, G. Kala, S. V. Kala, R. J. Barrios, G. M. Habib, D. J. Lukin, C. M. Danney, M. M. Matzuk, M. W. Lieberman, *Proc. Natl. Ac. Sci.* **2000**, *97*, 5101–5106.
[27] B. Yan, J. W. Smith, *Biochemistry* **2001**, *40*, 8861–8867.
[28] A. P. Wiita, S. R. Koti Ainavarapu, H. H. Huang, J. M. Fernandez, *Proc. Natl. Ac. Sci.* **2006**, *103*, 7222–7227.
[29] N. Wong Shi Kam, Z. Liu, H. Dai, *J. Am. Chem. Soc.* **2005**, *127*, 12492–12493.
[30] S. S. Agasti, C. C. You, P. Arumugam, V. M. Rotello, *J. Mater. Chem.* **2008**, *18*, 70–73.
[31] J. A. Dougan, C. Karlsson, W. Ewen Smith, D. Graham, *Nucl. Acids Res.* **2007**, *35*, 3668–3675.
[32] Z. Li, R. C. Jin, C. A. Mirkin, R. L. Letsinger, *Nucl. Acids Res.* **2002**, *30*, 1558–1562.
[33] B. C. Mei, E. Oh, K. Susumu, D. Farrell, T. J. Mountziaris, H. Mattoussi, *Langmuir* **2009**, *25*, 10604–10611.
[34] K. Susumu, H. T. Uyeda, I. L. Medintz, T. Pons, J. B. Delehanty, H. Mattoussi, *J. Am. Chem. Soc.* **2007**, *129*, 13987–13996.

Received: February 23, 2010
Published online: May 19, 2010